

## Study of neutron-rich nuclei using deep-inelastic reactions

I. Y. Lee, S. Asztalos, M.-A. Deleplanque, B. Cederwall,\* R. M. Diamond, P. Fallon, A. O. Macchiavelli, L. Phair, F. S. Stephens, and G. J. Wozniak  
Lawrence Berkeley National Laboratory, Berkeley, California 94720

S. G. Frauendorf  
Research Center Rossendorf, Dresden, Germany

J. A. Becker and E. A. Henry  
Lawrence Livermore National Laboratory, Livermore, California 94550

P. F. Hua and D. G. Sarantites  
Washington University, St. Louis, Missouri 63130

J. X. Saladin  
University of Pittsburgh, Pittsburgh, Pennsylvania 15260

C. H. Yu†  
University of Rochester, Rochester, New York 14627  
(Received 24 February 1997)

We have used the  $^{48}\text{Ca}+^{176}\text{Yb}$  reaction to study the population of high-spin states in neutron-rich nuclei by deep-inelastic reactions. Using Gammasphere, we observed gamma transitions from nuclei several neutrons richer than the target. Yrast states with spin up to 20 were populated in this reaction. High-spin states in  $^{175,177,178}\text{Yb}$  were observed. In this region of reduced pairing, a reference based on experimental data was used to derive experimental Routhians. Systematics of experimental Routhians in neutron-rich Yb nuclei compare well with cranked shell-model calculations. [S0556-2813(97)03608-X]

PACS number(s): 21.10.Re, 25.70.Lm, 25.70.Hi, 21.60.Ev

### I. INTRODUCTION

Neutron-rich nuclei are of particular interest since they might reveal new aspects of nuclear structure associated with an excess of neutrons, such as a neutron skin, a modified shell structure, and new modes of excitation. However, these nuclei are difficult to produce, particularly in high-spin states. Currently, nuclear high-spin states are produced almost exclusively by heavy-ion-induced fusion reactions and in a few cases by Coulomb excitation. Fusion reactions form compound nuclei with spin as high as  $70\hbar$ . However, with stable beams and targets, only neutron-deficient nuclei can be produced by fusion reactions. Coulomb excitation can be used to study stable nuclei. For deformed nuclei, states with spins up to  $30\hbar$  have been populated by Coulomb excitation. Neutron-rich nuclei in the mass region of  $100 < A < 150$  produced as fission fragments have been studied and states with spin as high as  $20\hbar$  were observed. So far, high-spin states in neutron-rich nuclei and most of the odd-even and odd-odd nuclei near the stability line have not been studied due to the lack of suitable nuclear reactions. Neutron-rich radioactive beams would be required to do this if fusion reactions are

used. However, using deep-inelastic reactions together with the new gamma-ray detector arrays, one expects to have enough sensitivity, in spite of the low cross sections, to form these nuclei at high-spin states. Indeed, these reactions have been shown to produce a high multiplicity of gamma rays [1], and in reactions of rare-earth beams with rare-earth targets, a multiplicity of 40 has been observed [2,3]. Neutron-rich nuclei such as  $^{177}\text{Tm}$ ,  $^{180}\text{Yb}$ , and  $^{184}\text{Lu}$  have been identified from  $\beta$ - $\gamma$  spectroscopy following reactions of Xe on W [4]. In addition, attempts have been made to use deep-inelastic reactions to produce and study high-spin states. States with spin up to 20 have been observed in an in beam study [5], and isomers with spin 10 have been identified in off-beam studies [6]. Since these reactions produce many final nuclei, some of them with a low cross section, a high-efficiency gamma-ray detector array, such as Gammasphere, is needed to resolve the cascades through high-fold coincidence measurements. This paper reports on the yield of neutron-rich nuclei and the population of high-spin states in a particular deep-inelastic reaction. High-spin states in neutron-rich  $^{175,177,178}\text{Yb}$  were observed. These data enable us to extend the study of the spin-alignment processes to neutron-rich Yb nuclei, and to compare our results with cranked shell-model calculations.

### II. EXPERIMENTAL METHOD

We have employed the reaction  $^{48}\text{Ca}+^{176}\text{Yb}$  at a beam energy of 250 MeV. The most neutron-rich stable isotopes of

\*Current address: Department of Physics, Royal Institute of Technology, S-10405 Stockholm, Sweden.

†Current address: Oak Ridge National Laboratory, Oak Ridge, TN 37831.

the projectile and target were used in order to enhance the production of neutron-rich nuclei. A self-supporting metallic target of  $^{176}\text{Yb}$  with an isotopic enrichment of 97.8% and a thickness of about  $1\text{ mg/cm}^2$  was bombarded with a beam of 2 pA from the 88-Inch Cyclotron at LBNL. This target was sufficiently thin to allow both the projectile- and target-like fragments to decay outside the target so that gamma rays from short-lived high-spin states can be observed as sharp lines after Doppler-shift correction. An annular silicon-strip detector with an inner diameter of 5 cm and an outer diameter of 10 cm placed 1.8 cm downstream from the target was used to detect the scattered fragments. This detector covered polar angles from  $55^\circ$  to  $67^\circ$  with 16 concentric strips on the front surface and the full range of azimuthal angles with 16 sectors on the back surface. The early implementation of Gammasphere with 36 detectors was used to detect the gamma rays. Coincidence events with at least one fragment and two Compton-suppressed gamma rays detected were taken at a rate of 1000/sec.

The particle detector detects either the projectile-like or the target-like fragment. The detector was placed such that its laboratory angular range of  $55^\circ$  to  $67^\circ$  which corresponds to a center-of-mass (c.m.) angular range of  $68^\circ$ – $82^\circ$  for the scattered projectile-like fragment covered the grazing angle of the reaction. Thus the detection of the projectile-like fragments selects events with nuclear interaction from small impact parameter collisions. On the other hand, the target-like fragment has a c.m. angular range of  $47^\circ$ – $70^\circ$  which is more forward and corresponds to larger impact parameters. The detected projectile-like fragment has an energy of about 180–200 MeV and the target-like fragment has a lower energy of 25–56 MeV. Thus the projectile-like products were identified from their higher energy detected in the Si detector and the velocity vectors of the target- and projectile-like product were calculated from the angles determined from the Si detector assuming a two-body reaction. The Doppler-shift correction of the gamma rays was based on these vectors and the direction of the gamma rays. To study the gamma rays from the target-like fragments, event-by-event Doppler correction was made using the velocity of the target-like fragments. In the resulting spectra, the gamma rays from the target-like fragments show up as sharp lines with a FWHM about 0.8% of the energy, and the gamma rays of the projectile-like fragments were smeared out over a range about  $\pm 9\%$  of the energy.

Two- and threefold gamma-ray-coincidence data were analyzed for the gamma rays from the target-like fragments. Gamma-ray spectra were obtained by single and double gating on transitions belonging to a gamma cascade. Gamma sequences from Er, Tm, Yb, and Hf nuclei have been identified from this data set. Figure 1 shows the spectra of even-even Yb nuclei from the twofold data. The low-spin transitions of  $^{176}\text{Yb}$  have more than  $10^5$  counts and the highest line observed is the  $14 \rightarrow 12$ . The spectrum of  $^{174}\text{Yb}$  has ten times fewer counts but the highest spin observed is 18. This indicates that the yield of  $^{176}\text{Yb}$  drops faster as a function of spin than the yield of  $^{174}\text{Yb}$ . The spectrum of  $^{172}\text{Yb}$  has ten times fewer counts than the spectrum of  $^{174}\text{Yb}$  and because of the low yield the spectrum is not clean. The main impurity peaks are due to  $^{176}\text{Yb}$  and  $^{177}\text{Yb}$  and a third set is not identified. Figure 2 compares the spectra of  $^{178}\text{Yb}$  from

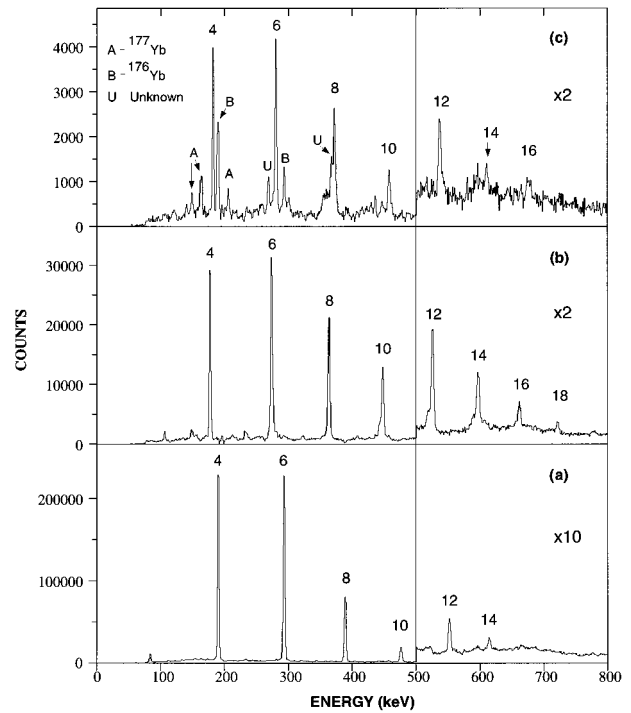


FIG. 1. Spectra from double- $\gamma$ -coincidence data corrected for the Doppler shift of the targetlike fragment for (a)  $^{176}\text{Yb}$ , (b)  $^{174}\text{Yb}$ , and (c)  $^{172}\text{Yb}$ .

single-gated twofold and double-gated triple data. The transitions belonging to  $^{178}\text{Yb}$  are clearly identified in the triples spectrum which is much cleaner than the doubles spectrum but with 1/6 of the counts. The identified impurity peaks in the double spectrum are from  $^{176}\text{Yb}$  and  $^{177}\text{Yb}$ . It is obvious

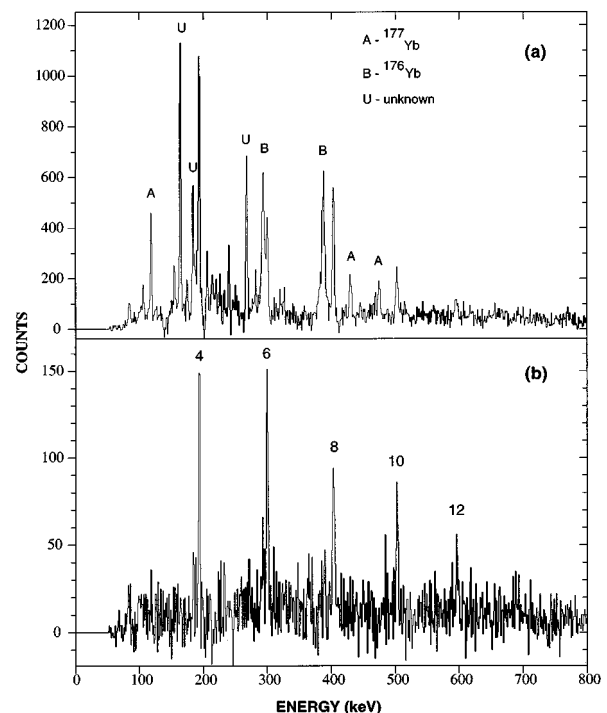


FIG. 2. Spectra of  $^{178}\text{Yb}$  from double (top) and triple (bottom)  $\gamma$  coincidence data with the Doppler correction for the targetlike fragment.



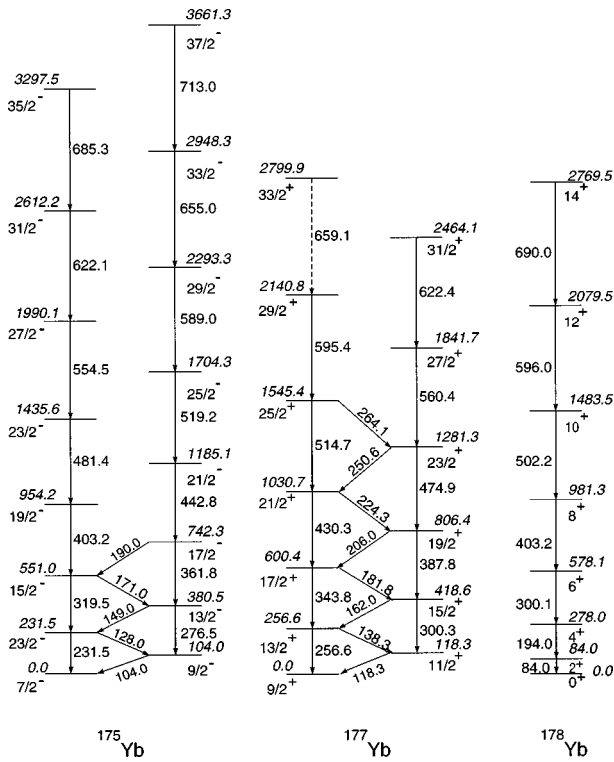


FIG. 6. The level schemes of  $^{175,177,178}\text{Yb}$  determined from this experiment. Previously, only three levels were known in each of these nuclei.

higher spin which is similar to that of the other Yb isotopes is most likely due to deep-inelastic reactions. Since few-nucleon transfer reactions do not bring in large amounts of angular momentum, the yield curve of Coulomb excitation plus few-nucleon transfer is expected to be similar to that of Coulomb excitation alone. The less steep yield curves of other nuclei also indicate that Coulomb excitation plus few-nucleon transfer are not important for the population of these nuclei which are indeed deep-inelastic products.

Before this study, only three levels in the yrast band were known in  $^{175,177}\text{Yb}$  and  $^{178}\text{Yb}$ . This work extends the yrast band of  $^{178}\text{Yb}$  to spin 12 and the yrast bands in  $^{175,177}\text{Yb}$  to spin 37/2 and 33/2, respectively. Based on coincidence relations, these new transitions are placed in the level schemes shown in Fig. 6. The structure of the yrast band of  $^{175}\text{Yb}$  is assigned [8] to be  $[514]7/2$  and the yrast band of  $^{177}\text{Yb}$  is based [9] on  $i_{13/2}[624]9/2$ . The spin and parity of the new states are based on these assignments and assuming the cascade transitions are of stretched  $E2$  in nature. One of the interesting properties of yrast levels with spin below about 20 in rare-earth nuclei is the alignment of a pair of neutrons in the  $i_{13/2}$  orbital. In the even-even nuclei, the aligned band crosses the ground-state band at a rotational frequency about 0.35 MeV. The interaction strength between the bands is expected to show an oscillatory behavior as the Fermi level moves through the multiplets of the  $i_{13/2}$  orbitals with different  $K$  values. In the odd neutron nuclei, if the odd neutron occupies an  $i_{13/2}$  orbital, the alignment is blocked. If the odd neutron does not occupy  $i_{13/2}$  orbitals, a band crossing similar to that of the even-even nuclei is observed.

The experimental results and comparison to the calculations are shown in Figs. 7–10. Figure 7 shows the moment of

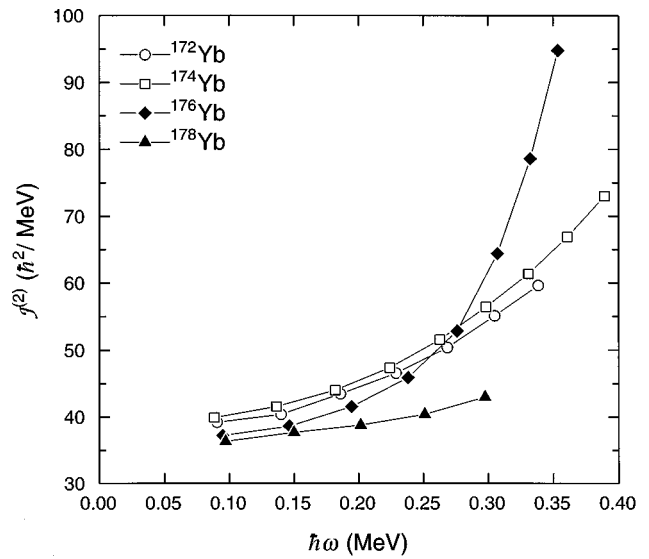


FIG. 7. Dynamic moment of inertia of even-even Yb nuclei.

inertia of the even-even Yb nuclei as a function of rotational frequency. The curves of  $^{172}\text{Yb}$  and  $^{174}\text{Yb}$  are similar to each other and  $^{176}\text{Yb}$  shows an increase of the moment of inertia at frequency above 0.25 MeV. The new results of  $^{178}\text{Yb}$  give a rather flat moment of inertia curve which suggests a smaller value for the interaction strength of the  $i_{13/2}$  neutron  $AB$  crossing than for the lighter Yb nuclei. The expected sharp backbend is likely to occur just above spin 12. It would be interesting to observe higher spin states with more statistics or using a reaction which makes products with higher angular momentum. However to explore the interaction strength, we need to study the Routhians which will be discussed below. Figure 8 shows the moment of inertia of the odd-mass  $^{175,177}\text{Yb}$ . The different behavior between these two nuclei is due to the fact that in  $^{177}\text{Yb}$  the odd neutron is occupying an  $i_{13/2}$  orbital and the alignment is blocked, producing a flat moment of inertia curve. For  $^{175}\text{Yb}$  the alignment of the  $i_{13/2}$  orbital is not blocked and its moment of inertia curve is similar to that of  $^{174}\text{Yb}$ .

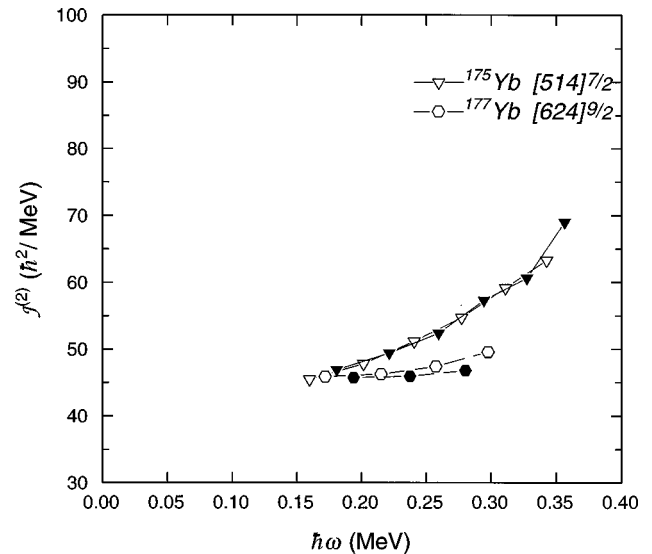


FIG. 8. Dynamic moment of inertia of  $^{175,177}\text{Yb}$ .

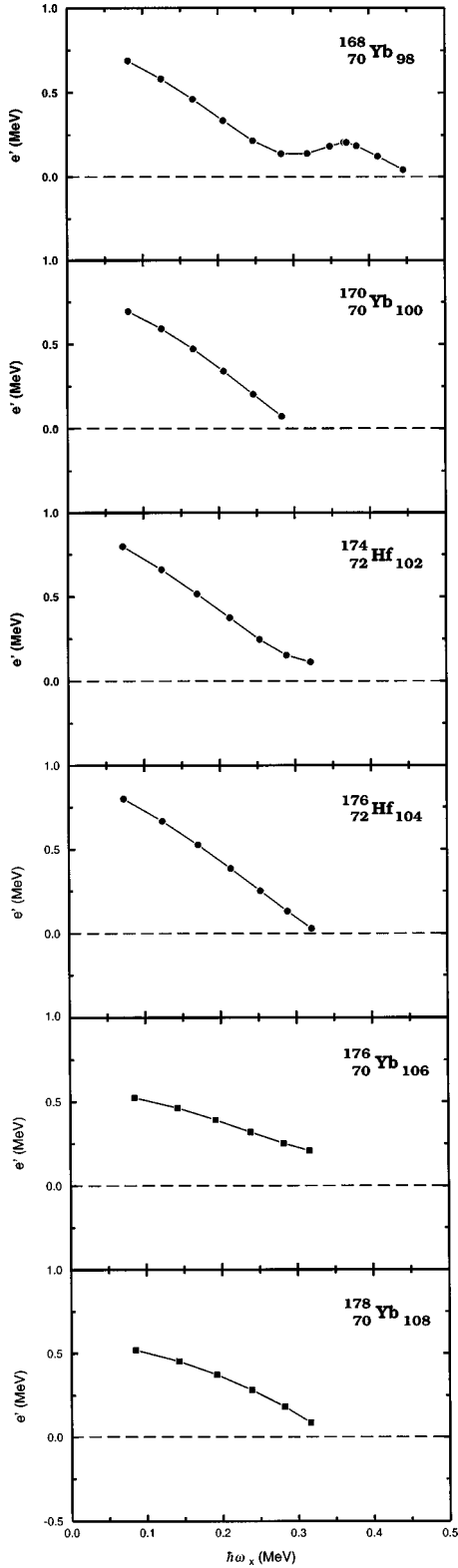


FIG. 9. Experimental Routhians for  $^{168,170}\text{Yb}$ ,  $^{174,176}\text{Hf}$ , and  $^{176,178}\text{Yb}$  as a function of  $\omega_x$ . They are obtained from the energy differences of yrast levels in even-even nuclei and the  $i_{13/2}$  band in the neighboring odd- $N$  nuclei.

To analyze the response of the  $i_{13/2}$  quasiparticles to rotation we compare the experimental Routhians with the ones calculated by means of the cranked shell model (CSM). We use the modified oscillator version and the associated param-

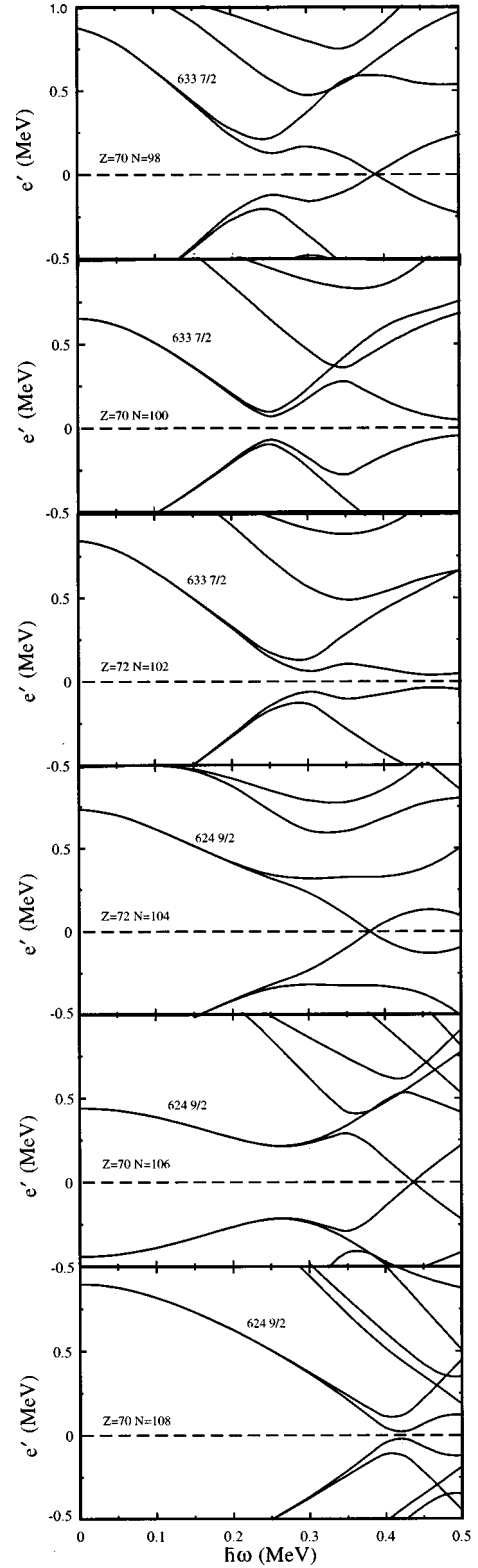


FIG. 10. Neutron Routhians from cranked shell-model calculations for  $^{168,170}\text{Yb}$ ,  $^{174,176}\text{Hf}$ , and  $^{176,178}\text{Yb}$ .

eters as described in Ref. [7]. The parameters of the rotating mean field are shown in Table I. The experimental  $i_{13/2}$  quasiparticle Routhians are shown in Fig. 9 and the calculated ones are shown in Fig. 10.

The experimental quasiparticle Routhians are obtained by subtracting from the experimental Routhian of the  $i_{13/2}$  band

TABLE I. Values of parameters [7] used in the cranked shell-model calculations.

Nucleus	$\varepsilon$	$\varepsilon_4$	$\Delta_n$ (MeV)
$^{174}\text{Yb}$	0.266	0.048	0.514
$^{176}\text{Yb}$	0.263	0.058	0.438
$^{178}\text{Yb}$	0.252	0.067	0.600
$^{174}\text{Hf}$	0.258	0.034	0.653
$^{176}\text{Hf}$	0.256	0.043	0.563

in the odd- $N$  nucleus the experimental Routhian of the even- $N$  neighbor, which is called the reference. This is different from the commonly used reference which is a fourth-order curve fitted to the low-frequency part of the measured Routhians (Harris fit). As discussed in detail in Ref. [7], such a “ $g$ -band reference” is only useful if one can clearly distinguish between the pieces of the band before and after the alignment of the pair of  $i_{13/2}$  quasiparticles. For very gradual structural changes, as in the heavy-Yb isotopes, it is more appropriate to apply the “yrast reference” of Ref. [7], which consists of the measured Routhians of the yrast states in the even- $N$  neighbor. The experimental quasiparticle Routhian obtained in this way can directly be compared with the lowest calculated  $i_{13/2}$  quasiparticle Routhian. Figure 9 shows the experimental quasiparticle Routhians for the neutron numbers  $N=98-108$ . These curves were obtained by using the yrast levels in  $^{168,170,176,178}\text{Yb}$  and the  $i_{13/2}$  bands in  $^{169,177}\text{Yb}$ . We had to use the data for  $^{174,175,176}\text{Hf}$  for  $N=102$  and  $104$ , because the  $i_{13/2}$  band in  $^{173}\text{Yb}$  is not observed.

For  $N=98$  and  $100$ , the calculated curves, lowest Routhians in Fig. 10, clearly show first an upbend of the quasiparticle Routhian, which represents the  $AB$  alignment in the even- $N$  nucleus (in the yrast reference), and a later down bend, which represents the  $BC$  alignment in the odd- $N$  nucleus. The large repulsion for  $N=98$  and the sharper crossing for  $N=100$  reflect the well-known oscillations of the interaction between the  $g$  and  $s$  bands as function of the neutron number [10,11]. These two neutron numbers correspond to the right side of the  $N=98$  maximum of the interaction strength. The measured Routhians compare well with the calculated ones.

Above  $N=102$ , the  $AB$  and  $BC$  crossings are no longer clearly discernible. Nevertheless, the calculated behavior seems to correlate with the experimental one. The case for  $N=102$  shows some slight up bend, corresponding to the

increased interaction at the  $AB$  crossing. For  $N=104$  the Routhian goes straight down heading for an intersection with the zero line. The calculated intersection occurs at somewhat higher frequency. For  $N=106$  the Routhian stays far from the zero line, whereas for  $N=108$  the experimental Routhian seems to head for an intersection with the zero line, both in accordance with the calculations. Obviously, the Routhians depend in a more complicated manner on  $N$  and  $\omega$  than discussed in Refs. [8] and [9] where just another oscillation of the interaction between the  $g$  and  $s$  bands around  $N=104$  is predicted. The reason is the rather low neutron pairing gap (the experimental value of  $\Delta_N$  lies around 0.6 MeV) as compared to the large spacing between the  $i_{13/2}$  levels (the spacing between the  $7/2$  and  $9/2$  levels is 1.3 MeV), which has the consequence that the crossings are no longer clearly separated [7]. Nevertheless, the comparison between calculated and experimental Routhians seems to indicate that the CSM is able to account for the quasiparticle response at low pairing in a quantitative way, if one compares directly the odd- with the even- $N$  bands (yrast reference), without trying to extrapolate the low-spin part of the even- $N$  bands as a Harris reference. This finding is certainly of interest for superdeformed bands where a similar weak pairing regime seems to be present.

In conclusion, we have established that with a high-efficiency gamma-ray array, it is possible to study high-spin states in neutron-rich nuclei produced in deep-inelastic reactions. These reactions extended the range of nuclei for high-spin structure study in the neutron-rich direction by about 10 neutron numbers. The observed variation in the experimental Routhians of the neutron-rich Yb nuclei agrees with the results of CSM calculations. We have shown that in this region of weak pairing and large interaction strength, it is necessary to use the experimental odd-mass  $i_{13/2}$  levels as a reference for calculating the experimental Routhians. With more powerful gamma-ray detector arrays being constructed, it will soon be possible to increase the sensitivity by a factor of 10. We are also planning to use a heavier projectile to bring more angular momentum into the products.

#### ACKNOWLEDGMENTS

The excellent beam provided by the staff of the 88-Inch Cyclotron is greatly appreciated. This work was supported in part by the U.S. Department of Energy under Contract Nos. DE-AC03-76SF00098 (LBNL), W-7450-ENG-48 (LLNL), and DE-FG02-88ER-40406 (Wash. U.).

- 
- [1] P. Glassel, R. S. Simon, R. M. Diamond, R. C. Jared, I. Y. Lee, L. G. Moretto, J. O. Newton, R. Schmitt, and F. S. Stephens, Phys. Rev. Lett. **38**, 331 (1977).
- [2] R. J. McDonald, A. J. Pacheco, G. J. Wozniak, H. H. Bolotin, L. G. Moretto, C. Schuck, S. Shih, R. M. Diamond, and F. S. Stephens, Nucl. Phys. **A373**, 54 (1982).
- [3] A. J. Pacheco, G. J. Wozniak, R. J. McDonald, R. M. Diamond, C. C. Hsu, L. G. Moretto, D. J. Morrissey, L. G. Sobotka, and F. S. Stephens, Nucl. Phys. **A397**, 313 (1983).
- [4] K. Rykaczewski, K.-L. Gippert, N. Kaffrell, R. Kirchner, O. Klepper, V. T. Koslowsky, W. Kurcewicz, W. Nazarewicz, E. Roeckl, E. Runte, D. Schardt, W.-D. Schmidt-Ott, and P. Tidemand-Petersson, Nucl. Phys. **A499**, 529 (1989).
- [5] H. Takai, C. N. Knott, D. F. Winchell, J. X. Saladin, M. S. Kaplan, L. deFaro, R. Aryaeieejad, R. A. Blue, R. M. Ronnigen, D. J. Morrissey, I. Y. Lee, and O. Dietzsch, Phys. Rev. C **38**, 1247 (1988).
- [6] R. Broda, R. H. Mayer, I. G. Bearden, Ph. Benet, P. J. Daly, Z.

- W. Grabowski, M. P. Carpenter, R. V. F. Janssens, T. L. Khoo, T. Lauritsen, E. F. Moore, S. Lunardi, and J. Blomqvist, Phys. Rev. Lett. **68**, 1671 (1992).
- [7] R. Bengtsson, S. Frauendorf, and F.-R. May, At. Data Nucl. Data Tables **35**, 15 (1986).
- [8] J. P. Mize, M. F. Bunker, and J. W. Starner, Phys. Rev. **100**, 1390 (1955).
- [9] K. W. Hoffmann, I. V. Krause, W. D. Schmidt-Ott, and A. Flammersfeld, Z. Phys. **160**, 201 (1966).
- [10] R. Bengtsson, I. Hamamoto, and B. Mottelson, Phys. Lett. **73B**, 259 (1978).
- [11] R. Bengtsson and S. Frauendorf, Nucl. Phys. **A314**, 27 (1979).